Journal of Anatomy

J. Anat. (2012) **221**, pp174–186 doi: 10.1111/j.1469-7580.2012.01523.x

Regional variations in the distribution and colocalization of extracellular matrix proteins in the juvenile bovine meniscus

Eric J. Vanderploeg,[1,3,‡] Christopher G. Wilson,[2,3,‡] Stacy M. Imler,[1,3] Carrie Hang-Yin Ling[4] and Marc E. Levenston[4]

[1]*George W. Woodruff School of Mechanical Engineering, Georgia Institute of Technology, Atlanta, GA, USA*
[2]*Wallace H. Coulter Department of Biomedical Engineering, Georgia Institute of Technology, Atlanta, GA, USA*
[3]*Parker H. Petit Institute for Bioengineering and Bioscience, Georgia Institute of Technology, Atlanta, GA, USA*
[4]*Department of Mechanical Engineering, Stanford University, Stanford, CA, USA*

Abstract

A deeper understanding of the composition and organization of extracellular matrix molecules in native, healthy meniscus tissue is required to fully appreciate the degeneration that occurs in joint disease and the intricate environment in which an engineered meniscal graft would need to function. In this study, regional variations in the tissue-level and pericellular distributions of collagen types I, II and VI and the proteoglycans aggrecan, biglycan and decorin were examined in the juvenile bovine meniscus. The collagen networks were extensively, but not completely, colocalized, with tissue-level organization that varied with radial position across the meniscus. Type VI collagen exhibited close association with large bundles composed of type I and II collagen and, in contrast to type I and II collagen, was further concentrated in the pericellular matrix. Aggrecan was detected throughout the inner region of the meniscus but was restricted to the pericellular matrix and sheaths of collagen bundles in the middle and outer regions. The small proteoglycans biglycan and decorin exhibited regional variations in staining intensity but were consistently localized in the intra- and/or pericellular compartments. These results provide insight into the complex hierarchy of extracellular matrix organization in the meniscus and provide a framework for better understanding meniscal degeneration and disease progression and evaluating potential repair and regeneration strategies.

Key words: collagen; extracellular matrix; fibrocartilage; meniscus; proteoglycans.

Introduction

The fibrocartilaginous knee menisci are instrumental in knee stability and load transmission, typically bearing 50–70% of the total load during normal knee joint motion (Shrive et al. 1978; Ghosh & Taylor, 1987) and contributing to joint lubrication (Fithian et al. 1990). Meniscal damage can occur concurrently with traumatic injuries to the anterior cruciate ligament, but can also be found in the absence of other signs of joint damage (Baker et al. 1985; Binfield et al. 1993; Roos et al. 1995). Meniscal tears have been associated with osteoarthritic degradation in the adjacent articular cartilage (Hough & Webber, 1990) and tears restricted to the avascular meniscal midsubstance typically fail to heal (King, 1990). Such cases are often not candidates for surgical repair using currently available techniques (Boyd & Myers, 2003), and even surgically repaired injuries that can heal with mechanically inferior tissue are prone to re-injury (Roeddecker et al. 1994). Full or partial meniscectomy following injury often results in the early onset of osteoarthritis (Roos et al. 1995, 1998; Cicuttini et al. 2002), at least partially due to dramatic changes in knee biomechanics in the absence of a competent meniscus. Therefore, opportunities exist to substantially improve the prospects for meniscal repair or regeneration.

Fabrication of engineered grafts for meniscal repair has proven challenging, in part because of the complex composition and organization of the extracellular matrix (ECM), which provides the necessary load-bearing and stress-

Correspondence
Marc E. Levenston, Department of Mechanical Engineering, Biomechanical Engineering, 233 Durand Building, Stanford, CA 94305-4038, USA. T: + 1 650 7239464; *F*: + 650 725 1587; *E: levenston@stanford.edu*
‡These authors contributed equally to this work.

Accepted for publication *10 May 2012*
Article published online *18 June 2012*

© 2012 The Authors
Journal of Anatomy © 2012 Anatomical Society

dissipating properties for these tissues to perform their biomechanical functions. Several collagen types, including types I, II, III, V and VI, are expressed in the meniscus but type I collagen is by far the most abundant, constituting 98% of the total collagen content (McDevitt & Webber, 1990). Collagen bundles in the radially middle and outer regions are primarily oriented circumferentially, parallel with the periphery of the tissue, whereas smaller, radially oriented 'tie' fibers are found along the surfaces and throughout the midsubstance of the menisci (Aspden et al. 1985; Skaggs et al. 1994; Petersen & Tillmann, 1998). The bundles consist primarily of type I collagen with type II collagen colocalizing around the tie fibers (Kambic & McDevitt, 2005). Immunostaining for type II collagen is more intense in the inner region than in the outer region of canine and ovine menisci (Kambic & McDevitt, 2005; Melrose et al. 2005). Type VI collagen is also abundant in the menisci, constituting approximately 1–2% of tissue dry mass (Wu et al. 1987), and has been reported to be found in the interterritorial and pericellular/cellular compartments of the ECM (McDevitt & Webber, 1990; Naumann et al. 2002).

Meniscal proteoglycans, including aggrecan, decorin, biglycan and perlecan, are also heterogeneously distributed (McDevitt & Webber, 1990; Melrose et al. 2005; Valiyaveettil et al. 2005; Smith et al. 2010). In adult porcine menisci, glycosaminoglycans constitute approximately 8% of the dry mass of the inner region but only 2% in the outer region (Nakano et al. 1997). Consistent with this finding, the core protein of the large proteoglycan aggrecan is more abundant in the inner regions than the outer regions of canine and ovine menisci (Melrose et al. 2005; Valiyaveettil et al. 2005). Finally, biglycan and decorin exhibit heterogeneous distributions in the adult rabbit menisci, with biglycan being more prevalent in the cartilaginous inner regions and decorin more prevalent with the fibrocartilaginous peripheral regions (Kavanagh & Ashhurst, 2001).

Previous studies have thus provided a substantial amount of information about the composition and organization of the ECM in meniscal fibrocartilage but few have leveraged the high-resolution imaging afforded by immunofluorescence microscopy to capture the fine details of ECM structure in the menisci. Additionally, few studies have assessed colocalization of various collagens and proteoglycans in these tissues. The objective of this study was to examine regional variations in the tissue-level and pericellular localizations of various collagens and proteoglycans in the juvenile bovine meniscus. The distribution and organization of collagen types I, II and VI and of the proteoglycans aggrecan, biglycan and decorin were imaged in menisci by immunofluorescence. Using detailed images, such as those presented here, insights can be gained into the intricacies of meniscal ECM structure and how various components of the ECM may interact to form this complex, composite tissue.

Materials and methods

Tissue specimen collection

Medial and lateral menisci were aseptically isolated from juvenile (2–4-week-old) bovine stifles (Research 87, Marlborough, MA) within 24 h of slaughter. Using a sterile scalpel, several 2–3 mm slices were taken from each meniscus in radial (coronal) and circumferential orientations (Fig. 1). The radial cross-sections allowed end-on imaging of the primary collagen network, and circumferential cross-sections allowed imaging along the main axis of these fibers. Several fixation and processing treatments were subsequently used to prepare meniscal tissue slices for imaging. Samples from two to three specimens per target molecule were imaged for these studies.

Scanning electron microscopy

Samples for scanning electron microscopy (SEM) were fixed overnight at room temperature using 2% glutaraldehyde and 2% paraformaldehyde in 0.1 M sodium cacodylate buffer (pH 7.3). After washing with the same buffer for 5 min, samples were post-fixed in 1% osmium tetroxide for 1.5 h, twice washed in deionized water for 5 min, and dehydrated in graded alcohols (30, 50, 70, 90, and 100% in 15-min steps). Samples were then dried with hexamethyldisilazane (50, 100 and 100%, 15–30 min per step) and sputter-coated with 100 Å of gold/palladium. Microstructural organization of an intact radial cross-section of a lateral meniscus and both radially and circumferentially oriented samples from a medial meniscus were examined with a variable pressure scanning electron microscope (Hitachi S-3400N; Hitachi High-Technologies Europe GmbH, Germany) operating at 10 kV. A composite image of the meniscal cross-section was assembled by tiling and registering individual low magnification images using the TrakEm2 plugin (Schmid et al. 2010) in IMAGEJ (version 1.46, National Institutes of Health).

Sample processing for localization of ECM proteins

Slices used for imaging of decorin or biglycan were fixed in 10% neutral buffered formalin (NBF) at 4 °C for 48 h, washed in phosphate-buffered saline (PBS), and stored in 70% ethanol until processing. The slices were embedded in paraffin, sectioned to 5 μm, mounted on positively charged slides, and deparaffinized through xylenes and graded alcohols. After rehydration, sections were permeabilized with 0.1% Triton X-100 for 15 min at room temperature, rinsed with PBS, and subjected to antigen retrieval with 0.125% trypsin for 20 min at 37 °C. Sections were blocked in a buffer with 1% bovine serum albumin (BSA), 0.1% gelatin, 2% normal goat serum and 0.05% Tween-20. The sections were incubated overnight at 4 °C with primary antibodies (Table 1; kind gifts from Dr Larry Fisher, NIDCR) diluted 1 : 100 in PBS containing 1% BSA and 0.1% gelatin. Sections treated with 10 μg/mL non-immune rabbit IgG (Sigma) served as negative controls. An Alexa Fluor® 488-conjugated secondary antibody (Table 1; 20 μg/mL in PBS, 1 h at room temperature) was used for detection and the sections were stained with DAPI to localize cell nuclei. These sections were mounted with Gel-Mount (Biomeda, Foster City, CA).

Slices used for the imaging of other ECM proteins were fixed in 10% NBF at 4 °C for 3–4 days. Slices were then sectioned to

© 2012 The Authors
Journal of Anatomy © 2012 Anatomical Society

Table 1 Antibodies used in immunolocalization studies

Antigen	Host	Fluorophore	Supplier/part number	Figures
Type I collagen	Mouse		Abcam/ab90395	5–7
Type I collagen	Rabbit		Abcam/ab292	3
Type II collagen	Rabbit		Abcam/ab300	3 & 5
Type VI collagen	Rabbit		Abcam/ab6588	3 & 6
Biglycan	Rabbit		Dr. Larry Fischer (NIDCR)/LF-96	4
Decorin	Rabbit		Dr. Larry Fischer/ LF-94	4 & 7
Aggrecan G1	Rabbit		Dr. John Sandy (Rush University)	4
Mouse IgG	Goat	Alexa Fluor® 594	Invitrogen/ A-11032	5–7
Rabbit IgG	Goat	Alexa Fluor® 488	Invitrogen/A-11008	3–7

50 μm, washed in PBS, and transferred to 1.5-mL microcentrifuge tubes. Antigen retrieval was accomplished using 0.25% trypsin in PBS for 30 min at 37 °C. Tissue sections were then treated with 1% Triton X-100 for 20 min at 37 °C and blocked with 2% normal goat serum in PBS for 10 min at room temperature. The sections were then incubated overnight at 4 °C with solutions of PBS plus 2% normal goat serum containing rabbit polyclonal antibodies against type I, type II or type VI collagen (Table 1) or the aggrecan G1 globular domain (a kind gift from Dr. John Sandy, Rush University Medical Center). All primary antibodies were used at a 1 : 50 dilution (20–100 μg/mL). Sections were washed with PBS and again blocked with 2% normal goat serum for 10 min at room temperature. Sections were incubated for 2–3 h at 4 °C with Alexa Fluor® 488-conjugated secondary antibodies (Table 1) diluted to 20 μg/mL in PBS and 0.1 lg/mL Hoechst 33258 to label cell nuclei, thoroughly washed in PBS, and mounted on microscope slides using Gel-Mount.

Sample processing for colocalization of collagens and proteoglycans

Slices used for simultaneous imaging of multiple ECM molecules were fixed in 10% NBF at 4 °C for only 4–6 h to prevent extensive cross-linking. The slices were then incubated in 30% sucrose at 4 °C overnight, transferred to cryomolds with Tissue-Tek O.C.T. embedding medium, and rapidly frozen in liquid nitrogen-cooled isopentane. Frozen tissue blocks were sectioned using a cryostat to 7 μm, transferred to SuperFrost plus microscope slides, and stored at −80 °C. Immediately prior to immunostaining, slides were dried at room temperature, fixed with acetone, and allowed to dry for at least 5 min before rehydration in PBS. Slides were transferred to Sequenza Slide racks (Thermo Shandon), washed with PBS, and treated with 0.1% Triton X-100 for 15 min at room temperature. Antigen retrieval was performed using 0.5% trypsin for 10 min at 37 °C and sections were blocked for 1 h at room temperature in PBS supplemented with 1% bovine serum albumin (BSA), 0.1% gelatin, 0.05% Tween-20, and 2% normal goat serum. Sections were then incubated for 1 h at room temperature with solutions of PBS plus 1% BSA and 0.1% gelatin containing combinations of primary antibodies. The use of a mouse monoclonal anti-type I collagen allowed staining in combination with rabbit anti-type II collagen, anti-type VI collagen, or anti-decorin. Dilutions of 1 : 100 (10–50 μg/mL) were used for all primary antibodies. Alexa Fluor 546- and Alexa Fluor® 488-conjugated secondary antibodies diluted 1 : 100 in PBS were added to the sections for 1 h at room temperature. Finally, DAPI was used to counterstain nuclei and coverslips were mounted on the slides using aqueous gel mounting medium. Negative controls were performed either by omitting primary antibodies from the immunostaining solutions or by substituting appropriate concentrations of non-immune mouse and rabbit IgG in place of primary antibodies.

Thick (50 μm) sections were imaged using a Zeiss LSM 510 laser scanning confocal microscope and thin (5–7 μm) sections were imaged using a Nikon Eclipse E400 epifluorescence microscope. Three color confocal images were acquired using argon (ex. 488 nm, green), helium-neon (ex. 543 nm, red) and argon (ex. 364 nm, blue) lasers. Epifluorescence microscopy images were acquired using individual filter cubes to view blue, green and red fluorescence signals. Images for each channel were captured individually with QCAPTURE PRO (Version 5.1, QImaging, Surrey, British Columbia) and later combined using IMAGEJ. Images for all samples for a given staining protocol were obtained using identical exposure times on the digital camera. All images presented here were obtained from medial menisci, but lateral menisci exhibited similar ECM molecule structure, organization and distribution.

Results

Matrix structure and organization

Low magnification SEM images of a radial cross-section of a lateral meniscus (Fig. 2A) revealed an intricate, contiguous matrix (arrows) surrounding the circumferential collagen bundles and merging with the meniscal surface layer (open arrow), consistent with previous reports (Petersen & Tillmann, 1998; Rattner et al. 2011). Higher magnification SEM images of radial (Fig. 2B–D) and circumferential (Fig. 2E–G) sections of a medial meniscus demonstrate that this surrounding matrix is composed of an intricate network of sub-micron fibers, both wrapping around and running parallel to the primary circumferential collagen bundles.

Localization of collagens I, II and VI

Confocal immunofluorescence microscopy revealed several interesting structural and organizational features of the collagen matrix (Fig. 3). Staining for type I collagen was diffuse in the inner region but appeared highly organized in the middle and outer regions (Fig. 3A–C). Large fiber bundles oriented perpendicular to the plane of the images were seen in the middle and outer regions (dashed ellipses in

© 2012 The Authors
Journal of Anatomy © 2012 Anatomical Society

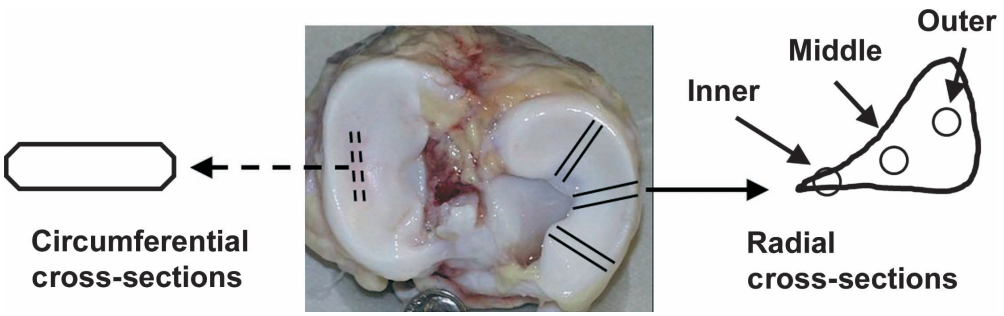

Fig. 1 Schematic illustrating meniscus partitioning into inner, middle and outer regions and orientation of radial and circumferential cross-sections.

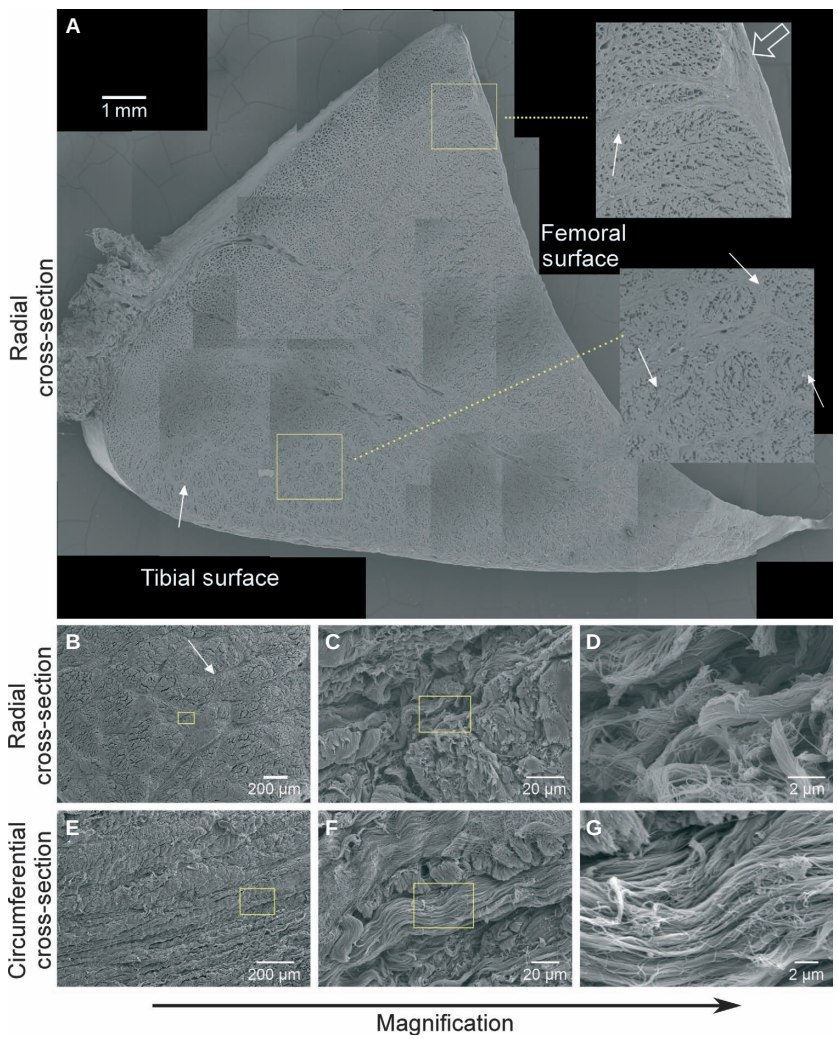

Fig. 2 Scanning electron microscopy of the juvenile bovine meniscus. A mosaic of images taken from a radial cross-section of a lateral meniscus (A) illustrates regional variations in the ultrastructure, including a contiguous fiber network (arrows) surrounding the circumferential fiber bundles. Scale bar: 1 mm. Insets (magnified three times, location indicated by boxes) show features of the ultrastructure near the femoral surface and the tissue interior, including merging of the fiber network (arrows) with the surface layer (open arrow). Note that holes within the circumferential bundles are processing artifacts. Progressively higher magnification images of radial (B–D) and circumferential (E–G) cross-sections from a medial meniscus depict the complex, anisotropic and hierarchical structure of the fibrillar extracellular matrix. Scale bars: 2–200 μm. Boxes indicate locations of the next higher magnification images. See Fig. 1 for orientations of radial and circumferential cross-sections.

© 2012 The Authors
Journal of Anatomy © 2012 Anatomical Society

Fig. 3B–C) as well as smaller fibers oriented parallel to the image plane in what are commonly referred to as radial tie fibers (arrowheads in Fig. 3B–C) (Skaggs et al. 1994; Kambic & McDevitt, 2005). Cells in these two regions were usually found at the junctions of the collagen fiber network and along the tie fibers.

Type II collagen staining had a spatial pattern similar to that seen for type I collagen (Fig. 3E–G). The inner zone exhibited diffuse, mostly unorganized type II collagen, although more intense staining was found pericellularly and near the tissue surface. The middle and outer regions contained a highly organized network of type II collagen fibers. In contrast to previous observations of mature canine menisci (Kambic & McDevitt, 2005), type II collagen was found throughout the cross-section of the bovine meniscus up to the outermost rim, with type II collagen being most prominent on the periphery of the large bundle structures (dashed ellipses in Fig. 3F–G).

Distinctions between type VI collagen staining and the other collagen molecules were evident (Fig. 3I–K). Type VI collagen was more organized in the inner region, with intense pericellular staining (block arrows), similar to its distribution in articular cartilage (Poole et al. 1988). However, type VI collagen also appeared to be organized in the interstitial areas between cells where discrete fibers of varying sizes often branched between multiple cells (Fig. 3I). Overall, the organization of type VI collagen staining in the middle and outer regions was similar to that seen for type I and II collagen, but a finer meshwork of fibers was visible. Type VI collagen was organized into larger bundles perpendicular to the image plane (dashed ellipse), but was also found in the intrabundle space as well as along radial tie fibers (arrowheads in Fig. 3J–K).

Finally, images of the collagen extracellular matrix from circumferential cross-sections (see Fig. 1 for image orientation) revealed further distinctions in meniscal collagen organization. Large, circumferentially oriented fibers, parallel to the image plane in this view, stained heavily for type I collagen (Fig. 3D), whereas smaller, similarly oriented fibers stained positive for type II and VI collagen (Fig. 3H,L). These smaller fibers typically had 10–20 μm spacing between areas of more intense staining. Nuclei were typically only found in areas that stained positively for type II or VI collagen and

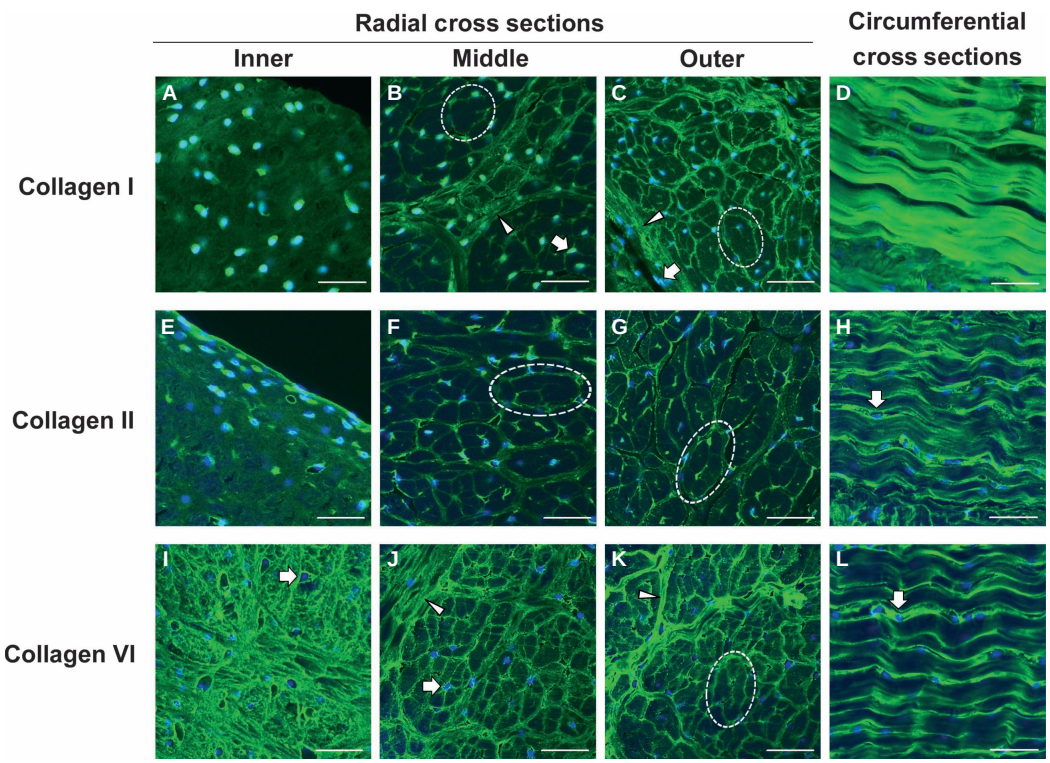

Fig. 3 Immunofluorescent localization of type I, II, and VI collagen in the juvenile bovine meniscus. Confocal laser scanning microscopy images of type I collagen (A–D), type II collagen (E–H), and type VI collagen (F–L) all exhibited regional variations within the meniscal tissue. The inner region exhibited diffuse staining for type I and II collagen, but intense pericellular and organized staining for type VI collagen. Collagen in the middle and outer regions was found to be organized in discrete fiber bundles, with type II and VI collagen at the periphery of the larger type I collagen structures (dashed ellipses). Sections aligned with circumferentially oriented fibers in the outer region of the meniscus exhibited intense staining for type I collagen, and type I and II collagen appeared to be concentrated around the type I collagen fibrils. Block arrows indicate regions of intense pericellular localization, and arrowheads point to radial tie fibers. Nuclei are labeled blue. Scale bars: 50 μm. See Fig. 1 for orientations of radial and circumferential cross-sections.

© 2012 The Authors
Journal of Anatomy © 2012 Anatomical Society

were often surrounded by staining for these proteins (block arrows). Negative controls without primary antibodies in the staining procedure exhibited little signal in all cases (not shown).

Localization of aggrecan, biglycan and decorin

Immunofluorescence imaging of aggrecan, biglycan and decorin demonstrated distinct pericellular and interstitial distributions of the large and small proteoglycans (Fig. 4). Consistent with a previous report on canine tissue (Valiyaveettil et al. 2005) and the localization of sulfated glycosaminoglycans in the meniscus (Fig. 4Q–S), the intensity of staining for the G1 domain of aggrecan was found to vary radially in coronal sections of the juvenile bovine meniscus (Fig. 4A–C). Aggrecan staining in the inner and middle regions was dense with additional localization in the pericellular matrix contributing to a semi-organized network interconnecting neighboring cells (block arrow in Fig. 4A,B). Staining intensity for interstitial aggrecan, distant from cell nuclei, was lower in the outer region but was found in an organized network that appeared to both surround large fiber bundles and subdivide them into smaller compartments (Fig. 4C). The pericellular matrix (i.e. near the nuclei) of outer zone cells was also intensely positive for aggrecan G1 (block arrow). Cell-level distributions of the small proteoglycans biglycan and decorin were both marked by intra- and/or pericellular staining observed throughout the meniscus (block arrows in Fig. 4D–O); the staining mainly appeared to demarcate individual cells and did not appear to be associated with an organized network as with the aggrecan staining. Staining of the inner and middle zone interstitial matrix was more diffuse for biglycan and decorin than for aggrecan, and weaker interstitial staining was observed for biglycan in the middle region than in the inner or outer regions of the meniscus. Biglycan (Fig. 4F,I) and decorin (Fig. 4L,O) staining in the outer regions of the meniscus revealed localization along tie fibers and other organized components of the interstitial ECM (arrowheads). Sections stained with non-immune IgG showed very weak background (Fig. 4P).

Colocalization of collagen I with other ECM constituents

Meniscus sections simultaneously immunostained for multiple matrix constituents provided additional insights into the relative locations of these four molecules. Sections co-stained for type I and II collagen produced images similar to those previously reported for mature canine tissue (Kambic & McDevitt, 2005). Colocalization of type I and II collagen was most striking in the outer zone, which contained large fiber bundles that stained positive for both collagen types as well as radial tie fibers, which stained somewhat diffusely for type I collagen, but more discretely for type II collagen (Fig. 5G–L). From the combined images it was evident that type II collagen appeared nearly everywhere that type I collagen was present, but type II collagen staining was more intense in the finer network of fibers that existed between larger circumferentially oriented fiber bundles.

Sections of the inner region co-stained for type I and VI collagen again showed an intricate network of type VI collagen and diffuse staining for type I collagen (Fig. 6A–F). The combined images indicated that there was some degree of colocalization throughout this region of the meniscus, but colocalization was most pronounced near fiber junctions (Fig. 6C,F). In the outer region, type I and VI collagen were predominately found to colocalize along large fiber bundles (Fig. 6G–L). Careful inspection revealed that these large fiber bundles stained positive for type I collagen across their entire thickness, whereas type VI collagen staining was most intense at the periphery (arrowhead in Fig. 6L). Additionally, more intense colocalization was found at fiber junctions, especially where multiple large fibers came together. Negative controls using non-immune IgG molecules in place of primary antibodies exhibited minimal signal for all tissue zones and sections imaged (not shown).

Co-staining of sections with antibodies for type I collagen and decorin demonstrated minimal colocalization of these ECM proteins in the inner region of the meniscus (Fig. 7). Decorin was found almost exclusively in the intra- and pericellular compartments in the inner region (block arrows), where type I collagen was localized diffusely throughout the tissue matrix. In contrast, decorin staining was intense in the intra- and pericellular space as well as at the periphery of the fiber bundles in the outer region. Colocalization with type I collagen was seen predominantly in the fibers of the interstitial space in the tissue, but rarely in the pericellular matrix.

Discussion

The composition and ultrastructure of the meniscal ECM give these tissues mechanical characteristics that are well adapted to performing their biomechanical roles (Ghosh & Taylor, 1987; Petersen & Tillmann, 1998). In addition to correlating meniscal mechanical properties with the organizational features of primary matrix constituents, efforts to understand the functional roles of less abundant ECM molecules have been ongoing (Adams et al. 1983; Eyre & Wu, 1983; McDevitt & Webber, 1990; Nakano et al. 1997). Although many ECM molecules have been identified in the meniscus, there remains a limited understanding of how these molecules may relate to and interact with one another. Thus, the goals of these studies were to investigate the fine structure of bovine meniscal tissue by electron and immunofluorescence microscopy and to explore the spatial relationships that exist between various ECM proteins.

Electron microscopy of the juvenile bovine meniscus provided high-resolution images of the primary collagen bun-

© 2012 The Authors
Journal of Anatomy © 2012 Anatomical Society

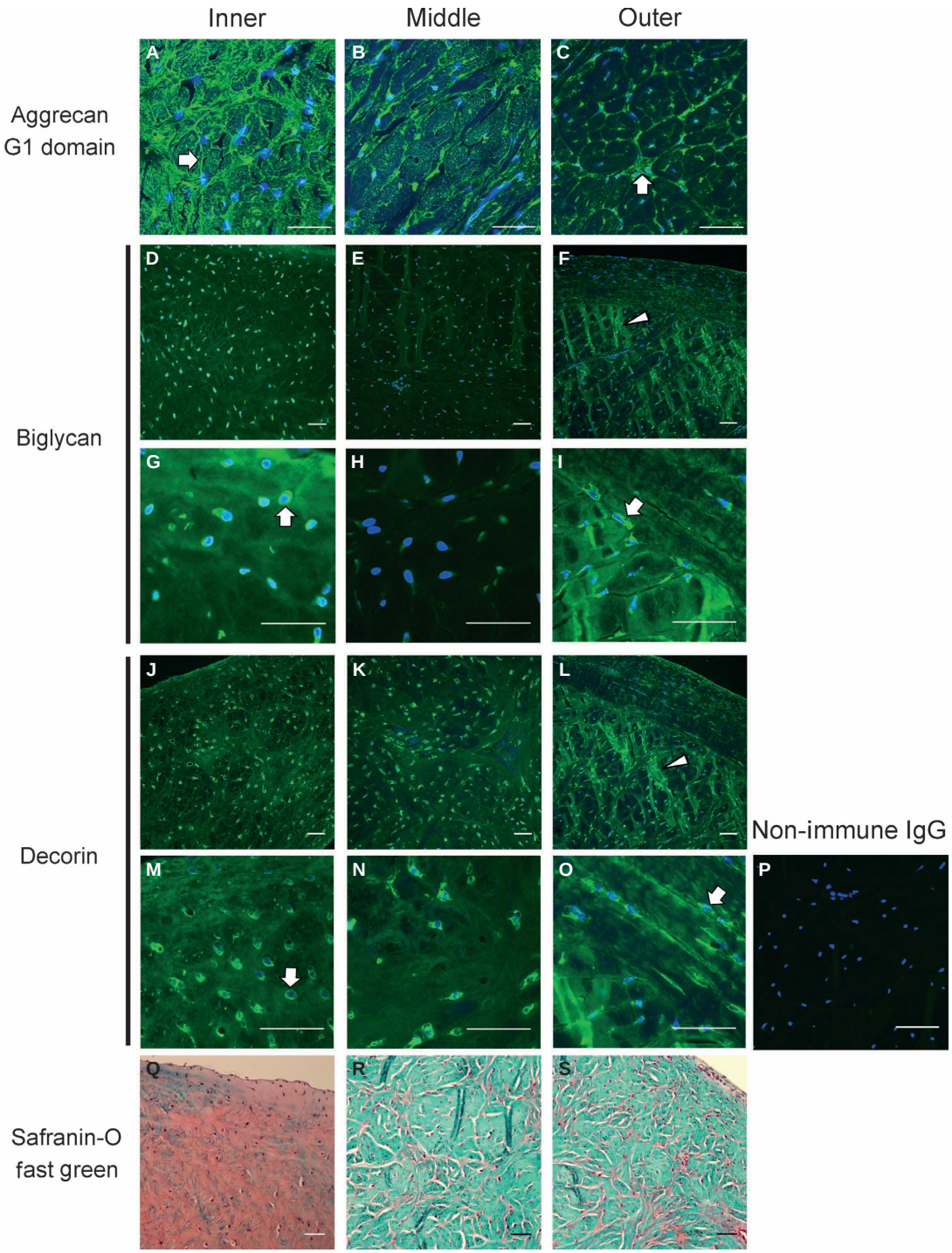

Fig. 4 Immunofluorescent localization of aggrecan, biglycan and decorin in the juvenile bovine meniscus. The G1 domain of the aggrecan core protein (A–C), imaged by confocal laser scanning microscopy in 50μm sections, is most densely localized in the inner region and more restricted to the margins of fiber bundles and the pericellular matrix in the middle and outer zones. The intensity of biglycan (D–I) and decorin (J–O) staining, imaged by epifluorescence microscopy of thin sections, is generally highest in the pericellular matrix (block arrows) throughout the meniscus, but radial tie fibers in the outer region also exhibit intense staining (arrowheads). Sections treated with non-immune rabbit IgG (p) in place of the primary antibody exhibited little background staining. Nuclei are labeled blue. Safranin-O/Fast Green stained sections (Q–S) are provided to illustrate the localization of sulfated glycosaminoglcyans and protein, respectively, for reference. Scale bars: 50 μm. All images are from radial cross-sections (see Fig. 1).

© 2012 The Authors
Journal of Anatomy © 2012 Anatomical Society

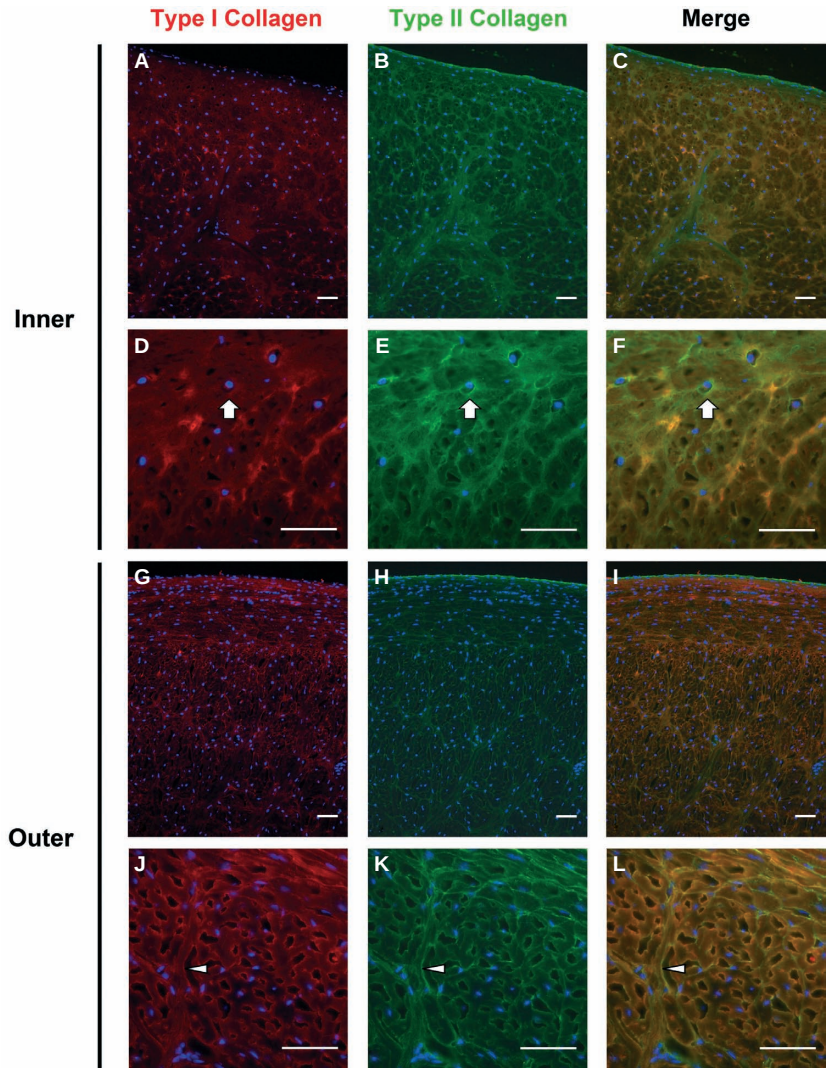

Fig. 5 Immunofluorescent colocalization of type I and II collagen in the juvenile bovine meniscus. Type II collagen was highly colocalized with type I collagen in both the inner (Q–F) and outer (G–L) regions of the meniscus, but type II collagen was more consistently localized in the pericellular compartment (block arrows). Nuclei are labeled blue. Arrowheads point to a tie fiber. Scale bars: 50 μm. All images are from radial cross-sections (see Fig. 1).

dles oriented circumferentially and radially throughout the tissue. Similar to previous studies with adult human meniscus (Petersen & Tillmann, 1998; Rattner et al. 2011), SEM images of the developing bovine meniscus show networks of matrix proteins that surround the primary bundles and contribute to the microenvironment of meniscal cells. This ultrastructural information provides an important context for, and indeed motivated, the studies aimed at identifying molecules that make up these networks.

The observed tissue localizations of type I and II collagen and aggrecan in our studies are consistent with proposed structure-function relationships of the meniscus where compressive forces that develop in the inner zone are primarily resisted by proteoglycans, and large circumferential tensile forces that develop in the outer zones are resisted by collagen fibers. Immunolocalization patterns for type I and II collagen were largely consistent with other published reports (Kambic & McDevitt, 2005; Chevrier et al. 2009; Killian et al. 2010). Type I collagen was found to be diffuse in the inner zone of medial menisci but was organized into large, circumferentially oriented bundles and radially directed tie fibers in the middle and outer zones. Our observations did differ from previous studies in that positive staining for type II collagen was seen well into the outer region of the juvenile bovine meniscus, whereas an abrupt loss of type II collagen signal has been reported in the outer zone of mature canine menisci (Kambic & McDevitt, 2005) and more gradual loss was seen in mature rabbit, sheep and human menisci (Chevrier et al. 2009; Killian et al. 2010). Although some decrease in type II collagen staining intensity in the outer zone was found in our studies, it was both subtle and gradual. These differences may be attributable to the age or species of the tissues and warrant further investigation. Our observation that type II collagen fibers seemed to surround the larger type I fibers in the outer zone of juvenile menisci suggests that this type II collagen may serve a transient role during developmental morphogenesis and tissue maturation. Performing similar immunofluorescence colocalization studies on tissue from older bovines would provide considerable insight into age- and species-specific

© 2012 The Authors
Journal of Anatomy © 2012 Anatomical Society

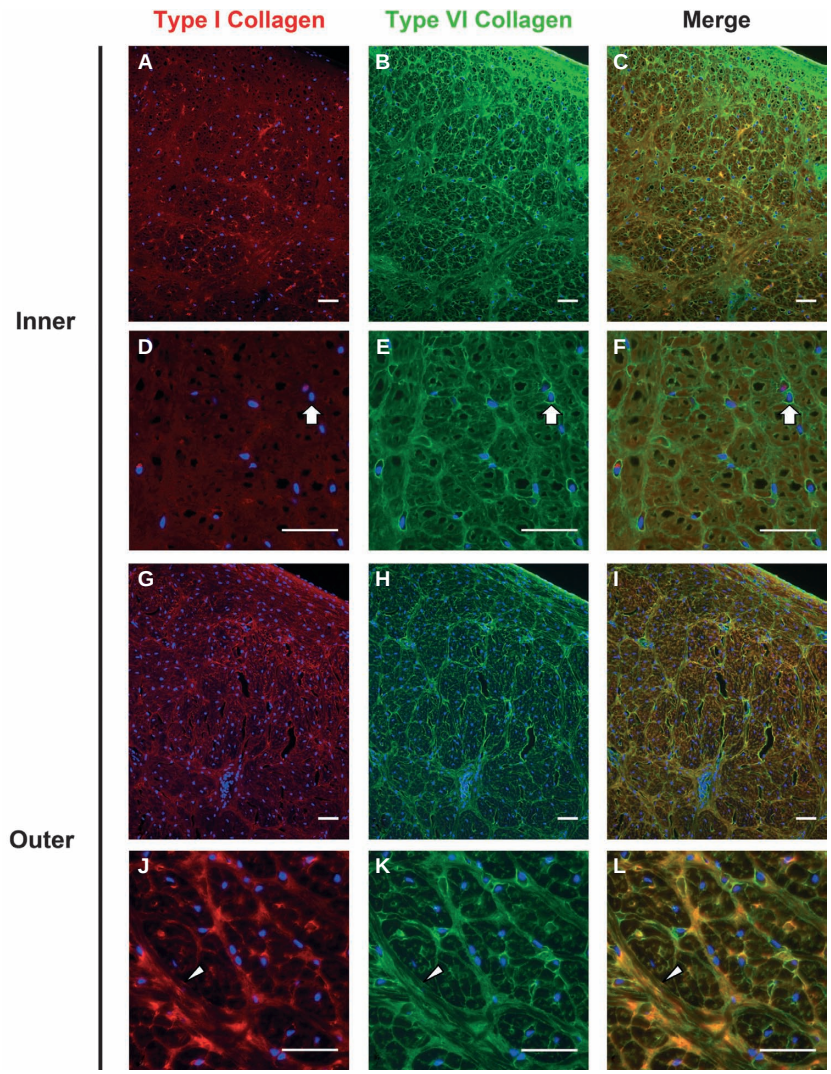

Fig. 6 Colocalization of type I and VI collagen in the juvenile bovine meniscus. The inner region (A–F) contained diffuse type I collagen staining and discrete pericellular (block arrows) and organized type VI collagen staining. Type I collagen was found in large, organized fiber bundles in the outer region (G–L) with type VI collagen located at the periphery of these bundles as well as pericellularly near fiber junctions. Nuclei are labeled blue. Arrowheads point to a tie fiber. Scale bars: 50 μm. All images are from radial cross-sections (see Fig. 1).

roles for type II collagen and other matrix proteins in the outer zone of the meniscus.

Type VI collagen is ubiquitous in connective tissues and has previously been identified in meniscus and other fibrocartilages (Wu et al. 1987; McDevitt & Webber, 1990; Felisbino & Carvalho, 1999). Both articular chondrocytes (Marcelino & McDevitt, 1995) and meniscal fibrochondrocytes (McDevitt et al. 1992) directly adhere to type VI collagen *in vitro*, and type VI collagen has been shown to bind a number of extracellular matrix molecules including type I and II collagen and decorin (McDevitt et al. 1991; Bidanset et al. 1992). Here, type VI collagen was immunolocalized in areas immediately surrounding resident cells as well as in an interconnected network with type I and II collagen throughout cross-sections of the tissue. Thus, this protein may serve to mechanically couple cells with large fiber bundles in the interterritorial matrix. The images presented here demonstrate that the pericellular matrix, and thus the local cellular microenvironment, is rich in type VI collagen throughout the meniscus.

Strong pericellular staining for type VI collagen appeared to be continuous with an intricate network of fibers colocalized around the periphery of large type I collagen fiber bundles that has not been previously described in detail. This structural hierarchy is similar to that seen in tendon fibrocartilages (Felisbino & Carvalho, 1999; Vogel & Peters, 2005; Carvalho et al. 2006) and may have functional implications for the meniscus during normal joint loading, degradation and repair. Type VI collagen has been localized at the surface of type I collagen fibrils in cell cultures and rat tail tendons (Bruns et al. 1986), suggesting a direct interaction between these collagens. Since type VI collagen is also known to interact with hyaluronan (McDevitt et al. 1991) and small proteoglycans (Bidanset et al. 1992), it may participate in the organization of these proteoglycans at the surface of type I collagen fibers. An organized proteoglycan network surrounding the collagen fiber bundles could both provide structural support during compressive loading and facilitate collagen sliding during tensile

© 2012 The Authors
Journal of Anatomy © 2012 Anatomical Society

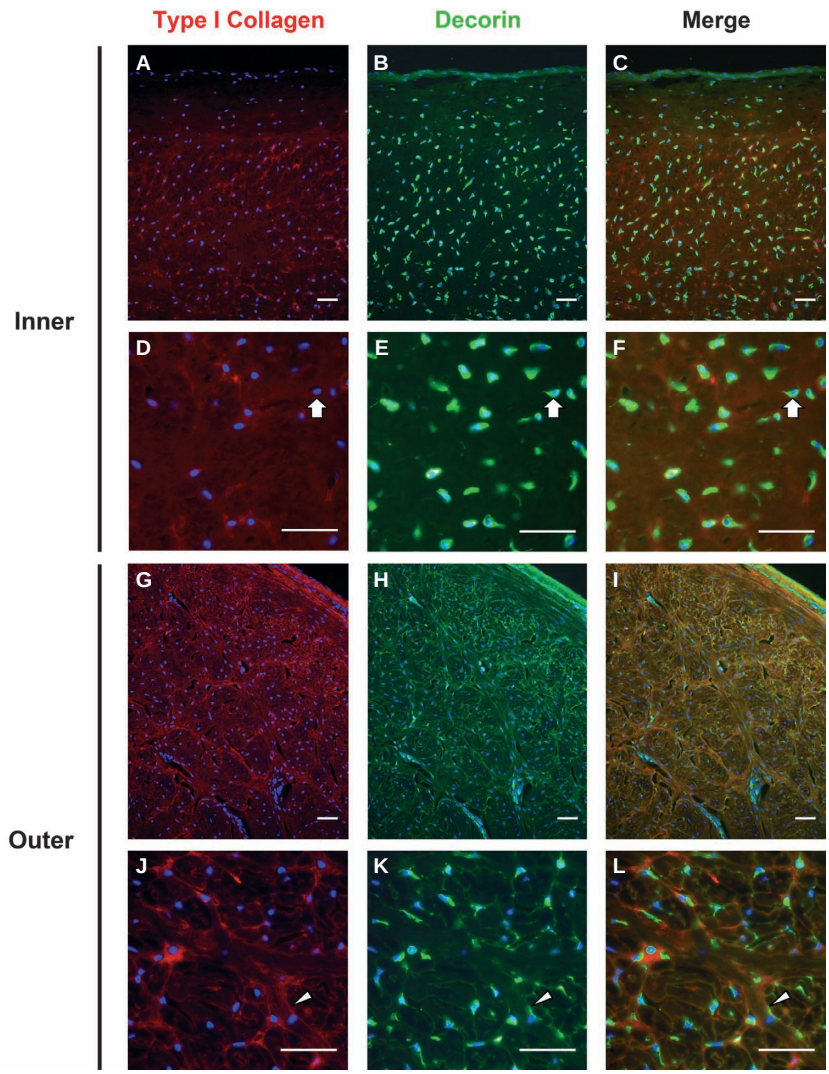

Fig. 7 Colocalization of type I collagen and decorin in the juvenile bovine meniscus. Staining for decorin was intense and nearly mutually exclusive of staining for type I collagen in the intra- and/or pericellular compartments (block arrows) of the inner region (A–F). In the outer region (G–L), decorin colocalized with type I collagen at the periphery of radial tie fibers (arrowheads) and near the surface of the tissue. Nuclei are labeled blue. Scale bars = 50 μm. All images are from radial cross-sections (see Fig. 1).

loading. Deletion of the *col6A1* gene in mice leads to reduced mechanical strength in the pericellular matrix of chondrocytes and an enhanced susceptibility to osteoarthritis (Alexopoulos et al. 2009), and it also disrupts the assembly of type I collagen fibrils in comparison with wild-type controls (Izu et al. 2011). Extending these types of studies to fibrocartilage tissues could help further elucidate the role of type VI collagen in various regions of the meniscus.

Staining for the G1 domain of the large proteoglycan aggrecan was intense and lacked extensive organization in the cartilage-like inner zone of the juvenile bovine meniscus. In contrast, the pattern of aggrecan G1 staining in the middle and outer zones was clearly defined by the collagen fiber bundles and progressively decreased in intensity towards the outer margin. This tissue-level distribution of aggrecan G1 is consistent with reports describing the proteoglycan distribution and aggrecan gene expression profiles in different zones of the meniscus (Nakano et al. 1997; Melrose et al. 2005; Valiyaveettil et al. 2005). Although the interstitial aggrecan in the inner zone of the meniscus is thought to provide compressive resistance, similar to its role in articular cartilage, the biomechanical function(s) of aggrecan in the outer zone is unclear. An emerging hypothesis is that large proteoglycans in the fibrocartilage of tendons (Vogel & Peters, 2005) and the intervertebral discs (Melrose et al. 2008) provide compressive stiffness as well as separation that allow collagen fibers to slide relative to one another during deformation. Aggrecan has been identified in tendons in remarkably similar patterns to those shown here for meniscus (Koob & Vogel, 1987; Vogel et al. 1994; Vogel & Peters, 2005). The organized network of aggrecan observed in the outer region of the meniscus, localized at the periphery of large, circumferentially-oriented type I collagen fiber bundles, could serve similar biomechanical roles in meniscal tissues, facilitating relative sliding and reorganization of the circumferential bundles to accommodate varying load patterns throughout the range of motion.

© 2012 The Authors
Journal of Anatomy © 2012 Anatomical Society

The functions of the aggrecan detected in the pericellular matrix are as yet unknown. As the cells in the middle and outer zones are located between the large fiber bundles or within the matrix subdividing these bundles, the locally elevated osmotic pressure generated by pericellular aggrecan may protect the cells from compressive deformation as the fiber bundles consolidate during loading. It is also important to note that detection of aggrecan G1 does not necessarily indicate the presence of highly glycosylated proteoglycan. Elevated densities of the aggrecan neoepitope NITEGE^{392}, generated by aggrecanases of the ADAMTS (a disintegrin and metalloproteinase with thrombospondin motif) family of proteases, have been reported in the middle and outer regions of the immature bovine meniscus (Wilson et al. 2009b) where pericellular localization of aggrecan G1 was most pronounced in images presented here, indicating that proteolytic processing of aggrecan is also region-specific in the juvenile bovine meniscus. In western blots of tissue extracts, an abundance of aggrecan bearing the G3 (C-terminal) domain was detected throughout the meniscus and the electrophoretic migration of these aggrecan species varied between inner, middle and outer regions (Wilson et al. 2009a). G3 fragments contain lectin domains that would afford retention in the tissue *via* interaction with extracellular glycoproteins such as tenascin C (Day et al. 2004) and fibulin (Aspberg et al. 1999), and such fragments and/or their complexes may have region-specific bioactivities or structural functions. Interestingly, another large proteoglycan, versican, was recently reported to be differentially expressed at the mRNA level in inner and outer regions of 6–12-month-old ovine meniscus (Fuller et al. 2012), and ADAMTS-mediated cleavage of versican generates fragments that regulate cell survival and differentiation (Kern et al. 2006; McCulloch et al. 2009). Defining the post-translational processing events and functions of proteoglycan fragments in the meniscus is beyond the scope of this report but it would provide considerable insight into the mechanisms by which cells in the meniscus assemble, maintain, and respond to regional variations in the ECM.

The small, leucine-rich proteoglycans biglycan and decorin were expressed throughout the juvenile bovine meniscus and were highly concentrated in the peri- and/or intracellular compartments. Similar to the meniscus, fibrocartilage from the adult human supraspinatus tendon exhibits minimal regional variations in the quantity of decorin core protein but exhibited more pronounced regional variation in the quantity of biglycan (Matuszewski et al. 2012); this finding adds to the growing body of evidence indicating highly conserved composition-function relationships among fibrocartilages. Biglycan and decorin bind, and thereby regulate the availability of, growth factors such as transforming growth factor-β_1 (Hildebrand et al. 1994). These interactions regulate the differentiation of mesenchymal and tendon progenitor cells *in vivo* (Bi et al. 2005, 2007) and aberrant matrix remodeling in fibrosis (Border et al. 1992; Isaka et al. 1996). These proteoglycans can also influence the morphology (e.g. fiber diameter) of collagen networks (Kuc & Scott, 1997; Corsi et al. 2002), and decorin and biglycan knockout mice exhibit marked changes in the mechanical properties of collagen-rich tissues including tendons and skin compared with wild-type controls (Danielson et al. 1997; Ameye et al. 2002). Thus, these small proteoglycans likely serve numerous functions related to regulation of cell phenotype and assembly and remodeling of the matrix in the meniscus (Izu et al. 2011).

The studies described here provide an in-depth investigation of the distribution and organization of several ECM proteins in the developing bovine meniscus. Differential organization patterns were seen in the inner and outer zones of the meniscus for aggrecan, and type I and II collagen. Although these molecules may constitute the bulk of the tissue matrix and provide much of the mechanical integrity in the meniscus, smaller constituents such as type VI collagen, decorin and biglycan are prominent in the intra- and pericellular space, suggesting a role in mechanical and biochemical signal transmission to meniscal cells. The ability to visualize the components of the meniscus using high magnification images produced with highly specific immunofluorescence techniques has provided insight into the potential function of these matrix molecules and how they may interact with one another and resident meniscal cells. Finally, efforts to better understand meniscal degeneration and to develop tissue engineered therapies for a diseased meniscus can be greatly enhanced by understanding the complexities of extracellular matrix organization and the composition of the local cellular microenvironment.

Acknowledgements

Supported by grant number R01AR052861 from the National Institute of Arthritis and Musculoskeletal and Skin Diseases (NIAMS) of the National Institutes of Health, the Cellular and Tissue Engineering Training Grant Program (C.G.W., NIH T32 GM008433-13), a National Science Foundation Graduate Research Fellowship and an ARCS Foundation Fellowship (E.J.V.). We thank Tracey Couse for assistance with preparation of the tissue sections.

References

Adams ME, Billingham ME, Muir H (1983) The glycosaminoglycans in menisci in experimental and natural osteoarthritis. *Arthritis Rheum* **26**, 69–76.

Alexopoulos LG, Youn I, Bonaldo P, et al. (2009) Developmental and osteoarthritic changes in Col6a1-knockout mice: biomechanics of type VI collagen in the cartilage pericellular matrix. *Arthritis Rheum* **60**, 771–779.

Ameye L, Aria D, Jepsen K, et al. (2002) Abnormal collagen fibrils in tendons of biglycan/fibromodulin-deficient mice lead to gait impairment, ectopic ossification, and osteoarthritis. *FASEB J* **16**, 673–680.

© 2012 The Authors
Journal of Anatomy © 2012 Anatomical Society

Aspberg A, Adam S, Kostka G, et al. (1999) Fibulin-1 is a ligand for the C-type lectin domains of aggrecan and versican. *J Biol Chem* **274**, 20444–20449.

Aspden RM, Yarker YE, Hukins DW (1985) Collagen orientations in the meniscus of the knee joint. *J Anat* **140** (Pt 3), 371–380.

Baker BE, Peckham AC, Pupparo F, et al. (1985) Review of meniscal injury and associated sports. *Am J Sports Med* **13**, 1–4.

Bi Y, Stuelten CH, Kilts T, et al. (2005) Extracellular matrix proteoglycans control the fate of bone marrow stromal cells. *J Biol Chem* **280**, 30481–30489.

Bi Y, Ehirchiou D, Kilts TM, et al. (2007) Identification of tendon stem/progenitor cells and the role of the extracellular matrix in their niche. *Nat Med* **13**, 1219–1227.

Bidanset DJ, Guidry C, Rosenberg LC, et al. (1992) Binding of the proteoglycan decorin to collagen type VI. *J Biol Chem* **267**, 5250–5256.

Binfield PM, Maffulli N, King JB (1993) Patterns of meniscal tears associated with anterior cruciate ligament lesions in athletes. *Injury* **24**, 557–561.

Border WA, Noble NA, Yamamoto T, et al. (1992) Natural inhibitor of transforming growth factor-beta protects against scarring in experimental kidney disease. *Nature* **360**, 361–364.

Boyd KT, Myers PT (2003) Meniscus preservation; rationale, repair techniques and results. *Knee* **10**, 1–11.

Bruns RR, Press W, Engvall E, et al. (1986) Type VI collagen in extracellular, 100-nm periodic filaments and fibrils: identification by immunoelectron microscopy. *J Cell Biol* **103**, 393–404.

Carvalho H, Felisbino S, Keene D, et al. (2006) Identification, content, and distribution of type VI collagen in bovine tendons. *Cell Tissue Res* **325**, 315–324.

Chevrier A, Nelea M, Hurtig MB, et al. (2009) Meniscus structure in human, sheep, and rabbit for animal models of meniscus repair. *J Orthop Res* **27**, 1197–1203.

Cicuttini FM, Forbes A, Yuanyuan W, et al. (2002) Rate of knee cartilage loss after partial meniscectomy. *J Rheumatol* **29**, 1954–1956.

Corsi A, Xu T, Chen XD, et al. (2002) Phenotypic effects of biglycan deficiency are linked to collagen fibril abnormalities, are synergized by decorin deficiency, and mimic Ehlers-Danlos-like changes in bone and other connective tissues. *J Bone Miner Res* **17**, 1180–1189.

Danielson KG, Baribault H, Holmes DF, et al. (1997) Targeted disruption of decorin leads to abnormal collagen fibril morphology and skin fragility. *J Cell Biol* **136**, 729–743.

Day JM, Olin AI, Murdoch AD, et al. (2004) Alternative splicing in the aggrecan G3 domain influences binding interactions with tenascin-C and other extracellular matrix proteins. *J Biol Chem* **279**, 12511–12518.

Eyre DR, Wu JJ (1983) Collagen of fibrocartilage: a distinctive molecular phenotype in bovine meniscus. *FEBS Lett* **158**, 265–270.

Felisbino SL, Carvalho HF (1999) Identification and distribution of type VI collagen in tendon fibrocartilages. *J Submicrosc Cytol Pathol* **31**, 187–195.

Fithian DC, Kelly MA, Mow VC (1990) Material properties and structure-function relationships in the menisci. *Clin Orthop* **252**, 19–31.

Fuller ES, Smith MM, Little CB, et al. (2012) Zonal differences in meniscus matrix turnover and cytokine response. *Osteoarthritis Cartilage* **20**, 49–59.

Ghosh P, Taylor TK (1987) The knee joint meniscus. A fibrocartilage of some distinction. *Clin Orthop* **224**, 52–63.

Hildebrand A, Romaris M, Rasmussen LM, et al. (1994) Interaction of the small interstitial proteoglycans biglycan, decorin and fibromodulin with transforming growth factor beta *Biochem J* **302** (Pt 2), 527–534.

Hough AJ Jr, Webber RJ (1990) Pathology of the meniscus. *Clin Orthop* **252**, 32–40.

Isaka Y, Brees DK, Ikegaya K, et al. (1996) Gene therapy by skeletal muscle expression of decorin prevents fibrotic disease in rat kidney. *Nat Med* **2**, 418–423.

Izu Y, Ansorge HL, Zhang G, et al. (2011) Dysfunctional tendon collagen fibrillogenesis in collagen VI null mice. *Matrix Biol* **30**, 53–61.

Kambic HE, McDevitt CA (2005) Spatial organization of types I and II collagen in the canine meniscus. *J Orthop Res* **23**, 142–149.

Kavanagh E, Ashhurst DE (2001) Distribution of biglycan and decorin in collateral and cruciate ligaments and menisci of the rabbit knee joint. *J Histochem Cytochem* **49**, 877–885.

Kern CB, Twal WO, Mjaatvedt CH, et al. (2006) Proteolytic cleavage of versican during cardiac cushion morphogenesis. *Dev Dyn* **235**, 2238–2247.

Killian ML, Lepinski NM, Haut RC, et al. (2010) Regional and zonal histo-morphological characteristics of the lapine menisci. *Anat Rec (Hoboken)* **293**, 1991–2000.

King D (1990) The healing of semilunar cartilages. 1936. *Clin Orthop Relat Res* **252**, 4–7.

Koob TJ, Vogel KG (1987) Site-related variations in glycosaminoglycan content and swelling properties of bovine flexor tendon. *J Orthop Res* **5**, 414–424.

Kuc IM, Scott PG (1997) Increased diameters of collagen fibrils precipitated in vitro in the presence of decorin from various connective tissues. *Connect Tissue Res* **36**, 287–296.

Marcelino J, McDevitt CA (1995) Attachment of articular cartilage chondrocytes to the tissue form of type VI collagen. *Biochim Biophys Acta* **1249**, 180–188.

Matuszewski PE, Chen YL, Szczesny SE, et al. (2012) Regional variation in human supraspinatus tendon proteoglycans: decorin, biglycan, and aggrecan. *Connect Tissue Res* doi: 10.3109/03008207.2011.654866.

McCulloch DR, Nelson CM, Dixon LJ, et al. (2009) ADAMTS metalloproteases generate active versican fragments that regulate interdigital web regression. *Dev Cell* **17**, 687–698.

McDevitt CA, Webber RJ (1990) The ultrastructure and biochemistry of meniscal cartilage. *Clin Orthop* **252**, 8–18.

McDevitt CA, Marcelino J, Tucker L (1991) Interaction of intact type VI collagen with hyaluronan. *FEBS Lett* **294**, 167–170.

McDevitt CA, Miller RR, Spindler KP (1992) The cells and cell matrix interactions of the meniscus. In: *Knee Meniscus: Basic and Clinical Foundations* (eds Mow VC, Arnoczky SP, Jackson DW), pp. 29–36. New York: Raven Press.

Melrose J, Smith S, Cake M, et al. (2005) Comparative spatial and temporal localisation of perlecan, aggrecan and type I, II and IV collagen in the ovine meniscus: an ageing study. *Histochem Cell Biol* **124**, 225–235.

Melrose J, Smith S, Appleyard R, et al. (2008) Aggrecan, versican and type VI collagen are components of annular translamellar crossbridges in the intervertebral disc. *Eur Spine J* **17**, 314–324.

Nakano T, Dodd CM, Scott PG (1997) Glycosaminoglycans and proteoglycans from different zones of the porcine knee meniscus. *J Orthop Res* **15**, 213–220.

© 2012 The Authors
Journal of Anatomy © 2012 Anatomical Society

Naumann A, Dennis JE, Awadallah A, et al. (2002) Immunochemical and mechanical characterization of cartilage subtypes in rabbit. *J Histochem Cytochem* **50**, 1049–1058.

Petersen W, Tillmann B (1998) Collagenous fibril texture of the human knee joint menisci. *Anat Embryol (Berl)* **197**, 317–324.

Poole CA, Ayad S, Schofield JR (1988) Chondrons from articular cartilage: I. Immunolocalization of type VI collagen in the pericellular capsule of isolated canine tibial chondrons. *J Cell Sci* **90**, 635–643.

Rattner JB, Matyas JR, Barclay L, et al. (2011) New understanding of the complex structure of knee menisci: implications for injury risk and repair potential for athletes. *Scand J Med Sci Sports* **21**, 543–553.

Roeddecker K, Muennich U, Nagelschmidt M (1994) Meniscal healing: a biomechanical study. *J Surg Res* **56**, 20–27.

Roos H, Adalberth T, Dahlberg L, et al. (1995) Osteoarthritis of the knee after injury to the anterior cruciate ligament or meniscus: the influence of time and age. *Osteoarthritis Cartilage* **3**, 261–267.

Roos H, Lauren M, Adalberth T, et al. (1998) Knee osteoarthritis after meniscectomy: prevalence of radiographic changes after twenty-one years, compared with matched controls. *Arthritis Rheum* **41**, 687–693.

Schmid B, Schindelin J, Cardona A, et al. (2010) A high-level 3D visualization API for Java and ImageJ. *BMC Bioinformatics* **11**, 274.

Shrive NG, O'Connor JJ, Goodfellow JW (1978) Load-bearing in the knee joint. *Clin Orthop* **131**, 279–287.

Skaggs DL, Warden WH, Mow VC (1994) Radial tie fibers influence the tensile properties of the bovine medial meniscus. *J Orthop Res* **12**, 176–185.

Smith SM, Shu C, Melrose J (2010) Comparative immunolocalisation of perlecan with collagen II and aggrecan in human foetal, newborn and adult ovine joint tissues demonstrates perlecan as an early developmental chondrogenic marker. *Histochem Cell Biol* **134**, 251–263.

Valiyaveettil M, Mort JS, McDevitt CA (2005) The concentration, gene expression, and spatial distribution of aggrecan in canine articular cartilage, meniscus, and anterior and posterior cruciate ligaments: a new molecular distinction between hyaline cartilage and fibrocartilage in the knee joint. *Connect Tissue Res* **46**, 83–91.

Vogel KG, Peters JA (2005) Histochemistry defines a proteoglycan-rich layer in bovine flexor tendon subjected to bending. *J Musculoskelet Neuronal Interact* **5**, 64–69.

Vogel KG, Sandy JD, Pogany G, et al. (1994) Aggrecan in bovine tendon. *Matrix Biol* **14**, 171–179.

Wilson CG, Nishimuta JF, Levenston ME (2009a) Chondrocytes and meniscal fibrochondrocytes differentially process aggrecan during de novo extracellular matrix assembly. *Tissue Eng Part A* **15**, 1513–1522.

Wilson CG, Vanderploeg EJ, Zuo F, et al. (2009b) Aggrecanolysis and in vitro matrix degradation in the immature bovine meniscus: mechanisms and functional implications. *Arthritis Res Ther* **11**, R173.

Wu JJ, Eyre DR, Slayter HS (1987) Type VI collagen of the intervertebral disc. Biochemical and electron-microscopic characterization of the native protein. *Biochem J* **248**, 373–381.

© 2012 The Authors
Journal of Anatomy © 2012 Anatomical Society